

A Correlation between Electrochemical Parameters and Stress Corrosion Cracking of Alloy 600 in High Temperature Caustic Solution

Jae Sun Baek, Jung Gu Kim
Sungkyunkwan University
300 Chunchun-dong, Jangan-gu, Suwon 440-746, Korea

Do Haeng Hur, Joung Soo Kim
Korea Atomic Energy Research Institute
150 Duckjin-dong, Yuseoung-gu, Daejeon 305-353, Korea

Abstract

The properties of the passive films formed on Alloy 600 at different applied potentials in 10% NaOH solution at 315°C was studied using in situ AC impedance and polarization measurements. The results were correlated with the stress corrosion cracking (SCC) behavior obtained from the C-ring tests in the same conditions. The change of the semiconductive property and the peak of relaxation time were observed at 0.2 V where the SCC rate showed a maximum. These results were also consistent with the prediction parameter for SCC obtained from fast and slow polarization scans.

Keywords: Caustic SCC, Alloy 600, EIS, Polarization, relaxation time constant

1. Introduction

Alloy 600 is an austenitic Ni-Cr-Fe alloy world widely used as a steam generator tube material of pressurized light water reactor nuclear plants. Since this alloy is known to be susceptible to stress corrosion cracking, the corrosion behavior has been extensively studied. Many of these studies have used sodium hydroxide solutions to simulate various caustic environments that can be formed in steam generator crevices between tube and tube sheet or tube and tube support plate.

One of the characteristic features of SCC of Alloy 600 in NaOH solutions is that the SCC rate is strongly dependent on the electrode potential. [1-4] That is, the crack depth is a maximum in the potential region just above the active-passive potential of the anodic polarization curve, while the crack depth decreases as the applied potential goes from in this potential region to in the active and passive region. This may suggest that the SCC mechanism of Alloy 600 in caustic environments be related to a film rupture process. Since according to

this the surface film plays a crucial role in the SCC process it is necessary to know the film properties such as the composition, structure and morphology of the anodic films formed at different potentials. To date, however, there is little information on the oxide properties with the potential. And there are also several studies on the change of the corrosion and the cracking modes of Alloy 600 in caustic solutions when the potential is controlled. Again, the previous authors did not consider the effect of the potential on the oxide properties.

In the present work, the effect of the potential on the properties of the oxide films formed on Alloy 600 in 10% NaOH solution at 315°C was studied using in situ AC impedance measurements. The results were discussed with the SCC behavior obtained using the C-ring specimens in the same experiment conditions. The relationship of a SCC parameter suggested by Fang and Staehle [5] to the SCC behavior was also examined.

2. Experimental

2.1. Test Material

A single heat of Alloy 600 steam generator tube with a 22.22 mm outer diameter and 1.23 mm wall thickness was used in all tests. Table 1 shows the chemical composition of this material. The tubing was mill annealed at 900°C for 10 minute. All tests were performed in 10 wt.% NaOH solution at 315°C, which was prepared using distilled de-ionized water and reagent grade NaOH.

Table 1. Chemical composition of Alloy 600 (wt.%)

C	Cr	Fe	Ni	Si	S	Mn	Cu
0.02	15.5	8.4	bal.	0.2	0.001	0.2	0.1

2.2. Electrochemical Measurements

Electrochemical tests were conducted in a nickel autoclave with a capacity of 1 liter. For electrochemical measurements, the tubing was longitudinally sectioned into four pieces, flattened and cut into a dimension of 5mm x 10mm. In order to make the electrical connection, an Alloy 600 lead wire was spot welded to the specimen, followed by shielding with heat-shrinkable polytetrafluoroethylene tube. Then the specimens were polished to 2000 grit SiC paper and cleaned in acetone before test. The reference electrode was made of nickel wire and the nickel autoclave body acted as the counter electrode. [6] Before heating the autoclave, the solution was deaerated by pressurizing to 1.38 MPa (200 psi) with 5% hydrogen-95% nitrogen gas followed by a slow depressurization. After this procedure was repeated three times, the mixed gas was continuously purged with a rate of 350 ml/min for 1 hour and was finally pressurized to 1.38 MPa as a cover gas.

In order to study the properties of the passive films, the electrochemical impedance spectroscopy (EIS) experiments were performed in the potential range from 0.12 V vs. Ni to 0.40 V vs. Ni after the specimen was pre-polarized at each potential for 2 hr. These impedance measurements were carried out using an potentiostat EG&G PAR model 273A and a frequency response analyzer Schlumberger model SI 1260 in the frequency range from 50 kHz to 10 mHz at 5 points/decade. The amplitude of the sinusoidal perturbation was 5 mV. The Z view software version 2.1 was used for data fitting of impedance spectra. In addition, to determine the relationship between the SCC parameter obtained from polarization curves and the SCC rate, polarization curves

were measured at two different scan rates of 20 mV/min and 1200 mV/min. All potentials were quoted with reference to the Ni electrode, unless otherwise noted.

2.3. Stress Corrosion tests

Stress corrosion cracking tests were performed using C-ring specimens. The specimens were prepared according to ASTM G38-73 and were stressed to a constant deflection of 1.50 mm (beyond yield strength) by means of Alloy 600 bolts and nuts. Three C-ring specimens were tested in each run using a 2-liter nickel autoclave with surfaces in the as-received conditions. The experiment processes were the same as used for electrochemical test except that the purging time is 1.5 hr. The specimens were potentiostatically polarized at 0.12, 0.15, 0.20, and 0.30 V anodic to the corrosion potential for 5 days. After each test, the specimens were sectioned through the middle of the C-ring and prepared for metallographic observation in order to determine the maximum depth and mode of attack.

3. Results and Discussion

3.1. SCC behavior

The relationship between the applied potential and crack growth rate is shown in Fig. 1. The crack growth rate shown is the average value based on the total testing time and the maximum crack depth. The specimens suffered SCC at all four potentials, with a maximum crack growth rate of about 9.7 $\mu\text{m/h}$ at 0.20 V. This potential dependency of SCC is well in accordance with the literatures reported by the previous investigators¹⁻⁴. In addition, the cracks were initiated at and propagated along grain boundaries regardless of the applied potentials, as shown in Fig. 2.

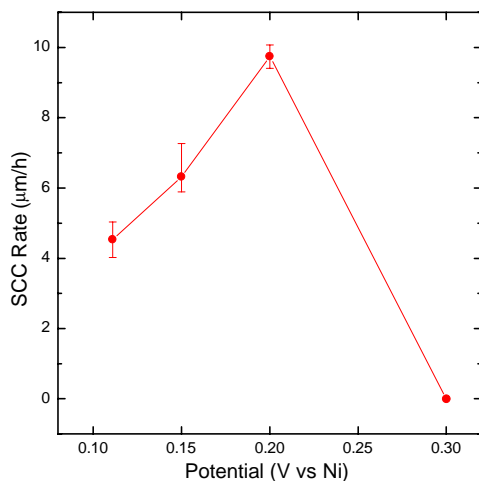


Fig. 1. Crack growth rate versus applied potential for Alloy 600 in 10 wt.% NaOH solution at 315 °C.

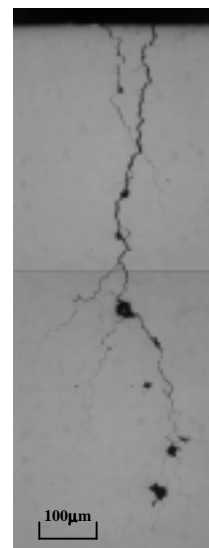


Fig. 2. Cross section of the SCC in C-ring held potentiostatically at 0.15V for 5 days in 10 wt.% NaOH solution at 315 °C.

3.2. Impedance results

The impedance spectra for anodic films formed on Alloy 600 electrodes in 10 wt.% NaOH solution are presented in Fig. 3. At potentials in the active-passive transition region as shown in Figs. 3 (a) and (b), the impedance bended over negative real axis in the low frequency range and an extra time constant due to the passivation process appeared. [7,8] However, in the passive region from 0.20 to 0.40 V, the spectra described loci in the fourth quadrant on the Nyquist plane as shown in Figs. 3 (c) ~ (f). These impedance data were analyzed by concerning two equivalent circuits in Fig. 4.

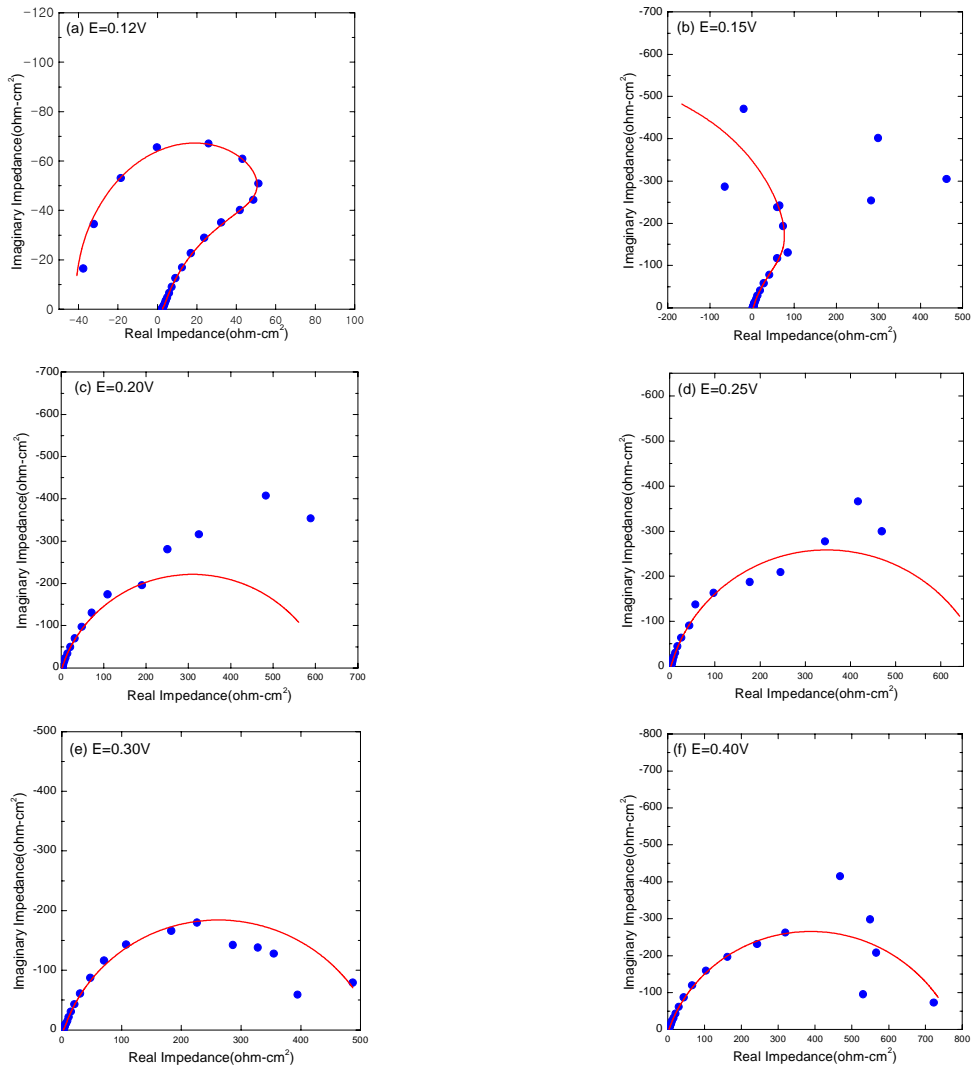


Fig. 3. The impedance data represented in Nyquist plots for Alloy 600 at the potentials given in the plots.

•: experiment, solid line: simulated diagrams using the equivalent circuit in Fig. 4. For the parameter values, see Table 2.

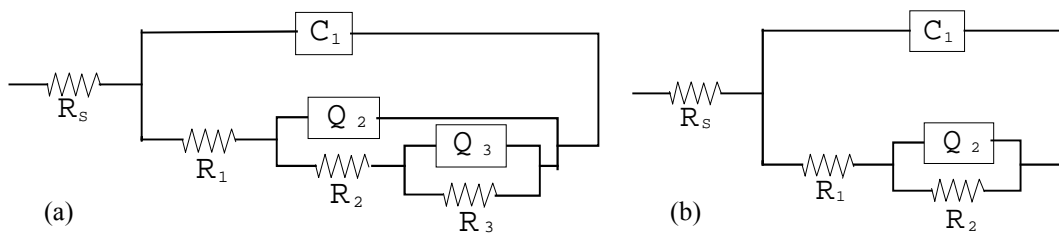


Fig. 4. Equivalent circuits of impedance measurements for Alloy 600 at different potential ranges: (a) active-passive region and (b) passive region.

The choice of these circuits were a compromise between a reasonable fitting of the experimental values, limited by the used software, and the maintenance of the number of circuit elements at a minimum, and still allows the association of these elements to the phenomena probably occurring at the electrode. These circuits involve a solution resistance R_s , two and (or) three parallel resistance-capacitance elements (R_1, C_1), (R_2, Q_2) and (or) (R_3, Q_3) taking into account a Cole-Cole distribution of relaxation time [7,9]. In such a model, the impedance of the capacitive element Q_i ($i= 2$ or 3) is presented by the so-called Constant Phase Element (CPE): $Z_{CPE} = [Q_i(j\omega)^n]^{-1}$ where the coefficient Q is a combination of properties related to the surface and electroactive species, j is $\sqrt{-1}$, ω is angular frequency, and n is the CPE exponent. The value of n can be used as a gauge of surface heterogeneity. Depending on the value of n , CPE represents resistance ($n=0$, $Q=R$), capacitance ($n=1$, $Q=C$), or Warburg impedance ($n=0.5$, $Q=W$). The impedance associated with the (R_2, Q_2) element in the network in Fig. 4 can be written as[7]

$$Z_2 = \frac{R_2}{1 + R_2 Q_2 (j\omega)^n} = \frac{R_2}{1 + (j\tau_2 \omega)^n} \quad (1)$$

where $(1-n)\pi/2$ is the angle between the real axis and the line to the center of the corresponding circle from the high-frequency intercept ($0 < n < 1$). The simulated data using the equivalent circuit in Fig. 4 is also superimposed in Fig. 3 for comparison. The data in low frequency range deviated from the simulated data, maybe due to instability of the electrode at the high temperature environment, so these data were not considered to calculate parameters of the equivalent circuits. All parameters of equivalent circuits were given in Table 2.

Table 2. Parameters of equivalent circuits for impedance measurement of Alloy 600 in 10 wt. % NaOH solution at various potentials.

E (V _{Ni})	R_s ($\Omega\text{-cm}^2$)	$C_1 \times 10^{-3}$ ($\Omega^{-1}\text{s}^n\text{cm}^{-2}$)	R_1 ($\Omega\text{-cm}^2$)	$Q_2 \times 10^{-3}$ ($\Omega^{-1}\text{s}^n\text{cm}^{-2}$)	n_2	R_2 ($\Omega\text{-cm}^2$)	$Q_3 \times 10^{-3}$ ($\Omega^{-1}\text{s}^n\text{cm}^{-2}$)	n_3	R_3 ($\Omega\text{-cm}^2$)
0.12	2.59	0.303	1.49	3.20	0.73	115.4	6.99	0.96	-160.9
0.15	2.59	0.306	2.34	1.57	0.77	447.1	0.96	1	-1268
0.20	1.99	0.444	0.93	2.70	0.76	621.8			
0.25	2.43	0.503	2.97	2.15	0.77	694.5			
0.30	2.59	0.410	3.56	2.38	0.75	538.1			
0.40	2.87	0.171	3.15	1.25	0.73	777.2			

3.2.1. The behavior of C_1 and R_1

Fig. 5 shows the dependence of the charge transfer resistance R_1 and the passive current density upon the potential. As can be seen from Fig. 5, despite the fact that the current density varied significantly with the potential, the charge transfer resistance R_1 does not vary remarkably with the potential, with an average value of about $2.4 \Omega\text{-cm}^2$. This suggests that the electrochemical reaction at the metal-oxide interface is a reversible interfacial charge transfer. [10]

Fig. 6 shows the potential dependence of $1/C_1^2$, which reveals Mott-Schottky behavior. In general, the

capacitance of a parallel-plate capacitor is related to the dielectric constant of the insulator, the area of the plate and the distance of separation between plates. Because the area of the electrode surface can be assumed to remain unchanged, the changes in the high frequency capacitance should be due to the changes in the dielectric constant of the layers and in the thickness of layers. [11] Therefore this capacitance C_1 seems to be related to the capacitance of a space charge layer in passive layer and its linearity to the potential supports the proposition that the space charge region dominates the measured high frequency impedance. In Fig. 6, two linear regions are apparent and can be related to the development of depletion layers promoted by band bending. The films behaved as a p-type semiconductor (negative slope) when they were formed below 0.25 V, while as an n-type semiconductor (positive slope) above this potential. However, the p-type semiconductivity is not so marked. The n-type passive film in which the Fermi level lies in the upper part of the forbidden energy gap, therefore, is more stable to corrosion than the p-type passive film in which the Fermi level is situated close to the valence band. The change in semiconductivity for the anodic films was in good agreement with the change in the SCC rate at 0.20 V in Fig. 1. Therefore the semiconductive properties of passive layers seem to be related to SCC.

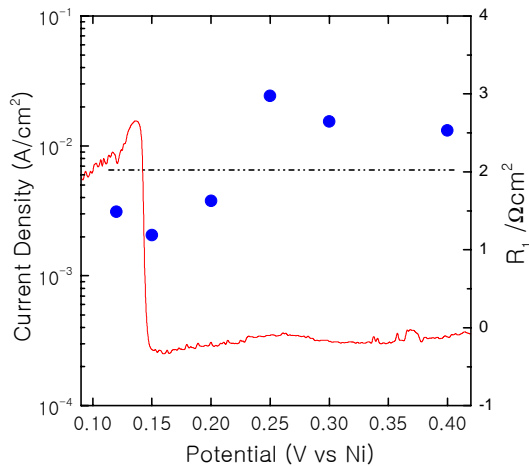


Fig. 5. The relation between potential and passive current density i (or resistance R_1) for passivated Alloy 600 in 10 wt.% NaOH solution at 315 °C. •: charge transfer resistance; solid line: current density

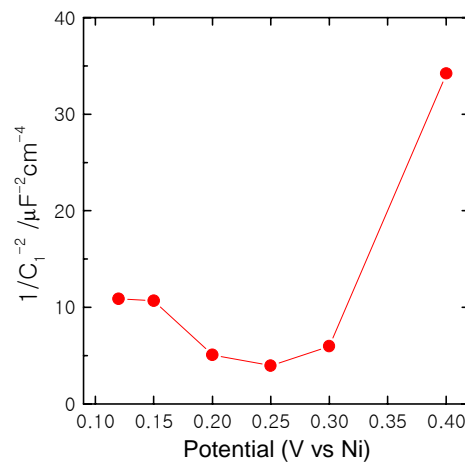


Fig. 6. Mott-Schottky plot of C_1 for passivated Alloy 600 in 10 wt.% NaOH solution at 315 °C.

3.2.2. The behavior of Q_2 and R_2

In Table 2, the Q_2 and n values indicated that this process did not show the pure capacitive behavior. It may be assumed that this capacitance would be exclusively related to the thickness relaxation of an underlying passivating film. Unfortunately the CPE values cannot be compared with each other since their dimensions depend on the value of n . But it is possible to identify the relaxation time constant (τ) from these values according to equation (1). This time constant τ can be related to the incremental passivation. The peak of τ , which varies with respect to the potential, has been found to occur when the dissolution rate equals to the passivation rate. [12-14] In Fig. 7 the maximum of τ at 0.20V corresponds to the maximum susceptibility of the SCC showed in Fig. 1. Therefore, this peak is directly related to SCC, and at the potential of maximum susceptibility to SCC the dissolution and passivation processes are balanced as to produce a favorable SCC

situation. So the presence of a peak in Fig. 7 associated with the second semicircles implies that the processes involved are involved in the mechanism of SCC.

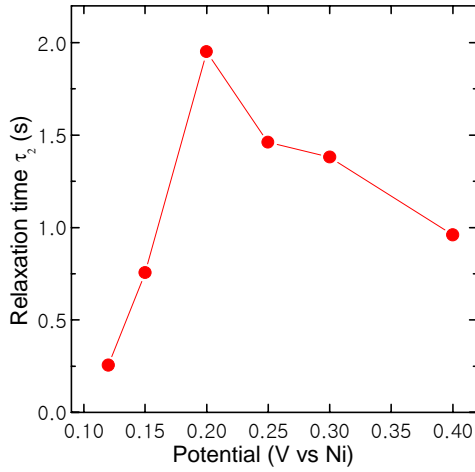


Fig. 7. The relation between potential and relaxation time τ_2 for passivated Alloy 600 in 10 wt.% NaOH solution at 315°C.

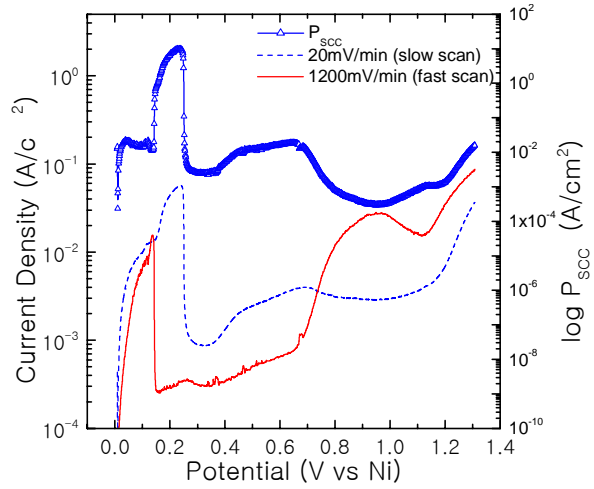


Fig. 8. Comparison of the fast and slow scanning polarization curves and SCC parameter P_{SCC} as a function of potential for alloy 600 in 10 wt.% NaOH solution at 315°C.

3.3. Comparison of result from slow/fast scanning rates

Fig. 8 shows the potentiodynamic polarization curves of Alloy 600 in 10wt.% NaOH at 315°C, measured with fast scan at 1200 mV/min and slow scan at 20 mV/min. An SCC parameter, P_{SCC} , proposed by Fang and Staehle [5] was also superimposed in this figure for comparison. Following Fang and Staehle [5], P_{SCC} is defined as

$$P_{SCC} = [R_{SR}(E)][i(E)_{1200mV/min}] = [R_{SR}^2(E)][i(E)_{20mV/min}] \quad (2)$$

where $R_{SR}(E)$ is the scanning rate ratio as a function of potential for current densities, i , determined at 1200mV/min and 20mV/min. Since this parameter is based on the hypothesis that the susceptibility to SCC could be correlated with the ratio of the current densities obtained from fast and slow polarization scans, high values of $P_{SCC}(E)$ should suggest the potential range be susceptible to SCC and thus indicate the transient instability of passive films. As can be seen in Fig. 8, the peak of $P_{SCC}(E)$ was observed in the potential range of around 0.20 V, where the SCC rate showed a maximum. Consequently, P_{SCC} seems to be used to predict the susceptible potential ranges for SCC of Alloy 600 in the present systems.

In summary, the maximum susceptible potential to SCC, the change of semiconductivity, the peak of time constant and P_{SCC} were observed at around 0.20 V. Therefore, it is important to note that these parameters drawn by in-situ EIS measurements can provide valuable insights into aspects of the SCC behavior at least in this experimental conditions. In addition, since all these parameters are correlated with the instability of films, it is suggested that the SCC mechanism of Alloy 600 in high temperature caustic is related to a film rupture process.

4. Conclusions

1. The peak in the relaxation time values was observed at 0.2 V where the SCC rate showed a maximum. Therefore, the relaxation times for Alloy 600 in caustic solutions could be the measure of the susceptibility to SCC.
2. The semiconductivity of passive film was changed from p-type to n-type at 0.25 V, near the maximum susceptible potential to SCC.
3. The potentiodynamic polarization technique with fast and slow scanning rates seems to provide a good correlation with the occurrence of SCC in this caustic solution.
4. The changes in semiconductivity, the P_{SCC} and relaxation time were correlated with the changes in the SCC resistance, suggesting that the SCC mechanism of Alloy 600 in caustic environments is related to the film rupture process.

Acknowledgements

This work has been carried out as a Steam Generator Materials Project of the Nuclear R&D program supported by the Ministry of Science and Technology.

Reference

- [1] N. Pessall, G.P Airey, and B.P. Lingenfelter, *Corrosion*, 35, 100 (1979).
- [2] N. Pessall, *Corrosion Science*, 20, 225 (1980).
- [3] R. Bandy, R. Roberge and D. Van Rooyen, *Corrosion*, 41, 142 (1985)
- [4] D. Van Rooyen and R. Bandy, EPRI Topical Report, NP-5129 (1987).
- [5] Z. Fang and R. W. Staehle, *Corrosion*, 55, 335 (1999).
- [6] J. R. Cels, *Corrosion*, 34, 198 (1978).
- [7] J. Ross Macdonald, "Impedance spectroscopy-Emphasising Solid Materials and Systems", Wiley, New York, 1987.
- [8] R. D. Armstrong and K. Edmondson, *Electrochimica Acta*, 18, 937 (1973).
- [9] M. W. Kendig, A. T. Allen and F. Mansfeld, *J. Electrochem. Soc.*, 131, 935 (1984).
- [10] X. P. Guo, Y. Tomoe, H. Imaizumi and K. Katoh, *J. Electroanal. Chem.*, 445, 95 (1998).
- [11] Shahed U. M. Khan and Wolfgang Schmickler, *J. Electroanal. Chem.*, 108, 329 (1980).
- [12] R. D. Armstrong and A. C. Coates, *Corrosion Science*, 16, 423 (1976).
- [13] R. D. Armstrong, *J. Electroanal. Chem.*, 34, 387 (1972).
- [14] R. D. Armstrong, M. F. Bell and J. P. Holmes, *Corrosion Science*, 19, 297, (1979).